ELSEVIER

Polymer 41 (2000) 7981–7992

polymer

www.elsevier.nl/locate/polymer

Synthesis and crystallization behavior of poly[5-(*N*,*N*-dimethylamino)-isoprene]

R. Bieringer*, V. Abetz

Makromolekulare Chemie II, Universität Bayreuth, D-95440 Bayreuth, Germany

In memoriam Prof. Dr Reimund Stadler

Received 12 January 2000; accepted 28 February 2000

Abstract

Anionic polymerization of *N*,*N*-dimethyl-2-methylene-3-buten-1-amine (5-(*N*,*N*-dimethylamino)-isoprene, DMAi) in toluene yields highly regio- and stereoregular polymers. The polymerization proceeds fast compared to non-polar dienes like butadiene or isoprene and polymers with almost exclusive *trans*-configuration are obtained. The amount of *trans*-connected monomer units is found to rise with decreasing polymerization temperature and with increasing molecular weight to a limiting value of about 95% at 25 kg/mol. Kinetic investigations reveal a polymerization behavior which does not follow simple first- or second-order kinetics with respect to monomer concentration. Poly[5-(*N*,*N*-dimethylamino)-isoprene] (PDMAi) synthezised in this way is semicrystalline with a degree of crystallinity of 55–60%. It shows a broad melting interval at 70°C besides a glass transition at −30°C. With the help of DSC, WAXS as well as cross-polarized light microscopy, the existence of two different crystal modifications is proven. The observed polymorphism is very similar to the one known from structurally related *trans*-polyisoprene (TPI).

Keywords: Synthesis and crystallization behavior; Anionic polymerization; Poly[5-(*N*,*N*-dimethylamino)-isoprene]

1. Introduction

The polymerization behavior of 2-substituted butadienes other than isoprene as well as the structure and properties of the resulting polymers have received increasing attention over the last 20 years. It has been known for a long time, that 2-substituted 1,3-dienes can be polymerized to form four constitutional isomeric microstructures. Using anionic polymerization techniques, the stereochemistry is found to depend on counter ion, solvent, monomer and chain end concentration as well as temperature and added polar modifiers [1]. Non-polar dienes typically give high amounts of 1,4-addition with lithium or lithium alkyls in bulk [2] or in non-polar solvents [3,4], whereas high vinyl contents are obtained using counter ions other than lithium [5,6], by polymerizing in polar solvents [7,8] or by adding polar modifiers [9–14]. An increase of steric hindrance of the non-polar side chain generally leads to higher degrees of 1,4-addition even in polar solvents [15–20]. 2-substituted dienes bearing amine functionalities have rarely been investigated to date. Interesting results from Nakahama et al. who analyzed the microstructures of a series of four different 2-[(*N*,*N*-dialkylamino)-dimethylsilyl]-1,3-butadienes in THF and in heptane [21] show that high amounts of 1,4-addition in THF (83–91%) and exclusive 1,4-addition in heptane with the ratios of *cis*/*trans*-addition varying with chemical structure are achieved.

2. Experimental section

2.1. Materials

5-(*N*,*N*-dimethylamino)-isoprene was prepared from isoprene by bromination followed by dehydrohalogenation yielding 2-bromomethyl-1,3-butadiene and subsequent nucleophilic substitution with dimethylamine. The monomer was purified by fractionated destillation as well as degassing and condensing onto dried dibutylmagnesium (1.0 M solution in heptane, Aldrich) and stirring under a N_2 inert atmosphere for 1 h. Toluene (p.a., Merck) was purified the same way by degassing and condensing onto dried dibutylmagnesium in a N_2 inert atmosphere followed by stirring for several hours. Both monomer and solvent were then condensed into a glass ampoule for transfer into the reaction vessel. *Sec*-butyllithium (1.3 M solution in

* Corresponding author.

0032-3861/00/$ - see front matter
PII: S0032-3861(00)00166-X

Table 1
Reaction conditions of the polymerizations of DMAi in toluene

Temperature (°C)	$[M]_0$ (mol l^{-1})	$[I]_0/10^{-3}$ (mol l^{-1})	$10^{-3} \times [I]_0/[M]_0$
+20	0.24	1.1	4.58
+6	0.18	0.8	4.44
−35	0.22	1.0	4.55

cyclohexane/hexane, Acros) was used without further purification.

2.2. Polymerization procedure

Anionic polymerizations were carried out in a 1000 ml stirred glass reactor (Buechi) with a thermostated cooling jacket under N_2 inert gas atmosphere. Monomer and solvent were added via glass ampoule and brought to the desired polymerization temperature. The required amount of *sec*-butyllithium was charged via syringe through a rubber septum. Through a small capillary outlet equipped with a tap, small portions of the reaction solution could be taken off the reactor in the course of the polymerization. After removal of solvent and unreacted monomer under reduced pressure conversions were determined by gravimetric analysis. The polymerizations were terminated by addition of 1 ml of degassed methanol. The polymer solutions were precipitated in acetone yielding colorless powdery polymer in all cases. 2–3 reprecipitation cycles were carried out in acetone after redissolution of the polymer in THF. Yields were always quantitative.

3. Characterization

^1H and ^{13}C NMR spectra were obtained using a Bruker AC 250 spectrometer (250 MHz for ^1H-nuclei, 62.9 MHz for ^{13}C-nuclei). The $CDCl_3$ solutions had concentrations between 25 and 70 mg/ml for ^1H- and 120–250 mg/ml for ^{13}C-spectra. All NMR measurements were carried out at 298 K using tetramethylsilane as internal standard.

Size exclusion chromatography (SEC) was performed on a WATERS system with refractive index and UV (254 nm) detection, using polyester filled columns (Gr_am columns from Polymer Standard Service, PSS) with pore sizes of 100, 3×10^3 and 10^4 Å and a particle size of 10 μm. The elution solvent was THF, the flow rate being 1 ml/min in all cases. A relative calibration with standard polystyrenes was used.

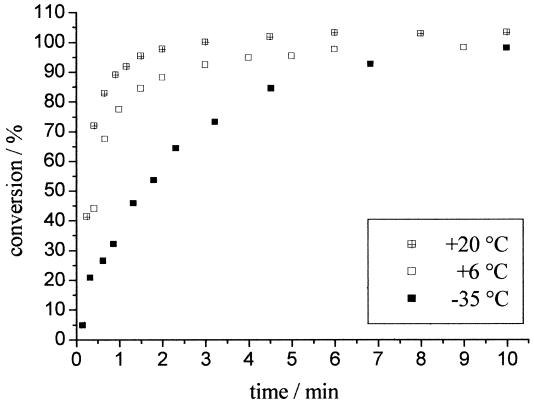

Fig. 1. Time-conversion plots of DMAi polymerizations at different temperatures.

Membrane osmometry was carried out on an Osmomat 090 from Gonotec at 35°C in toluene using a membrane of regenerated cellulose with a cut-off molecular weight of 20 kg/mol.

Differential scanning calorimetry (DSC) was accomplished by using a Perkin–Elmer DSC-7 instrument after calibration with chloroform and indium. Glass transition temperatures were taken at the inflection points and extrapolated to a heating rate of 0 K/min. Melting and crystallization temperatures were determined from their peak maxima.

Wide angle X-ray scattering (WAXS) was carried out on a D 8 Advance from Bruker AXS (40 kV, 40 mA) using CuK_α-radiation. Measurements were performed on 1 mm thick films at an angle interval of $5° < 2\theta < 60°$ in theta–theta geometry on reflection at room temperature.

Small angle X-ray scattering (SAXS) was carried out on a Bruker AXS Nanostar (40 kV, 40 mA) using CuK_α-radiation and a 2D-detector at an angle interval of $0.15° < 2\theta < 4.50°$. Measurements were performed on 1 mm thick films in vacuum at room temperature in transmission.

Transmission electron microscopy (TEM) was performed on a CEM 902 transmission electron microscope from Zeiss with an accelerating voltage of 80 kV. Sample preparation involved cryosectioning of the solvent cast film at −60°C followed by staining with OsO_4.

Cross-polarized light microscopy was carried out with an Orthoplan II Pol BK microscope from Leitz with a camera MPS 11 from Wild attached to it. A drop of a 5 wt% solution of the polymer under investigation was freed from dust and isothermally crystallized on a glass slide on a Mettler FP82HT hot stage.

Atomic force microscopy (AFM) was accomplished using a Dimension 3100 microscope from Digital Instruments in the tapping mode. The samples used were identical with the ones used in light microscopy experiments.

4. Anionic polymerization of 5-(*N*,*N*-dimethylamino)-isoprene (DMAi)

Satisfying results of the anionic polymerization of DMAi can only be obtained in non-polar solvents. The use of THF, diethyl ether, 1,4-dioxane, triethylamine or non-polar solvents with additives such as *N*,*N*,*N*′,*N*′-tetramethylethylendiamine (TMEDA) or crown ethers seems to slow down the polymerization in a way that high conversions are not achievable even after days [22,23]. This behavior is remarkably different from other anionically polymerizable

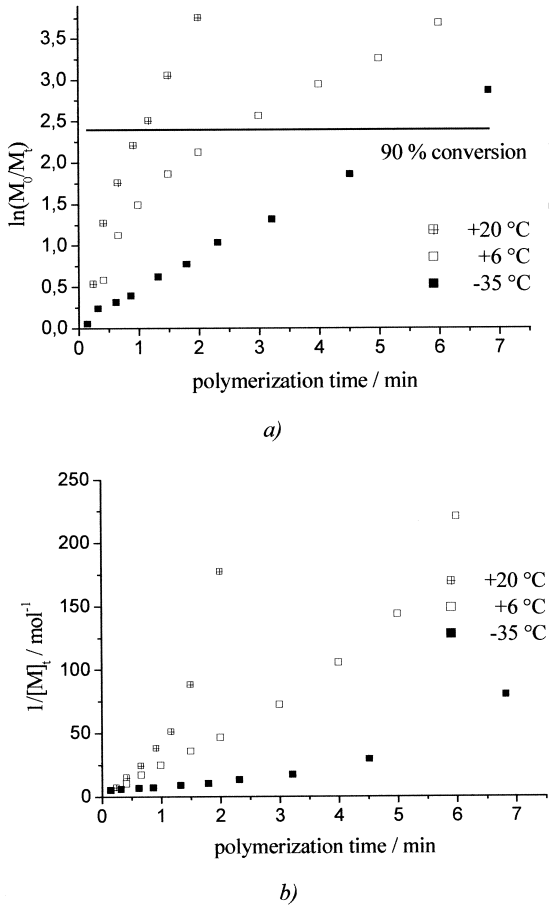

Fig. 2. Analysis of polymerizations of DMAi assuming (a) first-order kinetic behavior; and (b) second-order kinetic behavior with respect to monomer concentration.

monomers as enhanced charge separation between the living chain end and counter ion in polar solvents usually accelerates the growth rate. So far no satisfying explanation has been put forward.

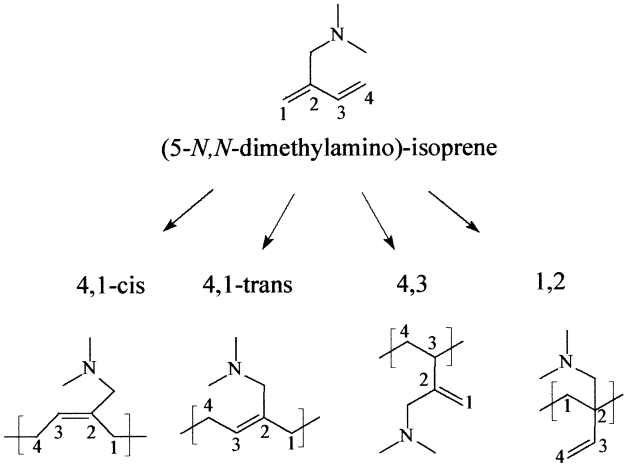

Fig. 3. Possible ways of DMAi addition onto the growing chain end.

4.1. Results

4.1.1. Polymerization kinetics

Sec-butyllithium initiated polymerizations of DMAi in toluene were carried out at three different temperatures while keeping the concentration of monomer $[M]_0$ and the ratio of initiator/monomer $[I]_0/[M]_0$ constant. Table 1 lists the details of these polymerizations. During the course of the polymerizations, small portions were taken from the reaction mixtures to determine the conversion by gravimetric analysis. The results are shown in Fig. 1.

The polymerizations proceed quickly with their rate increasing with increasing temperature, as expected. At a polymerization temperature of 20°C full conversion is already obtained after 2 min, while at a temperature of −35°C, the polymerization is finished after 15 min. The living anion is completely colorless as long as polymerization temperatures do not exceed −20°C, otherwise a yellow color occurs. Its intensity varies with temperature and which disappears instantaneously after termination of the polymerization with methanol.

Generally, non-polar dienes follow polymerization kinetics which are first order in monomer concentration in non-polar solvents as well as with added Lewis bases or in polar solvents [1]. The polarity of the solvent, besides influencing the rate constant, usually only effects the order by which the concentration of active species enters the kinetic equations. The equation $\ln([M]_0/[M]_t) = k_{app}t$ with the apparent rate constant $k_{app} = \bar{k}_p[P^*]$, where $[P^*]$ denotes the concentration of active centers and $\bar{k}_p$ is the true rate constant (generally being the mean of all involved rate constants), describes the polymerization as being first order in monomer concentration. Because it has been possible in the past to describe the polymerization kinetics of DMAi in *n*-hexane by assuming a second-order kinetic behavior with respect to monomer concentration [23] this was also attempted here. $1/[M]_t - 1/[M]_0 = k_{app}t$ describes this second-order dependence.

As can bee seen from Fig. 2, the polymerization kinetics can be fitted neither by assuming first- nor second-order kinetic behavior with respect to monomer concentration.

4.1.2. Microstructure

The influence of both temperature and monomer/initiator ratio on the obtained microstructure in the anionic polymerization of DMAi in toluene initialized with *sec*-butyllithium was investigated in detail.

In principle, four different ways of monomer addition are conceivable in the polymerization of DMAi as shown in Fig. 3. The designation follows the one used in polyisoprene polymerization, where '4,1' and '4,3' indicates the attack of the living anion at carbon 4 of the monomer.

^{1}H NMR spectroscopy allows to differentiate and quantify these four different ways of monomer linkage. As can be seen from Fig. 4, only one distinct signal appears in the vinylic region between 4.5 and 6.0 ppm which is due to

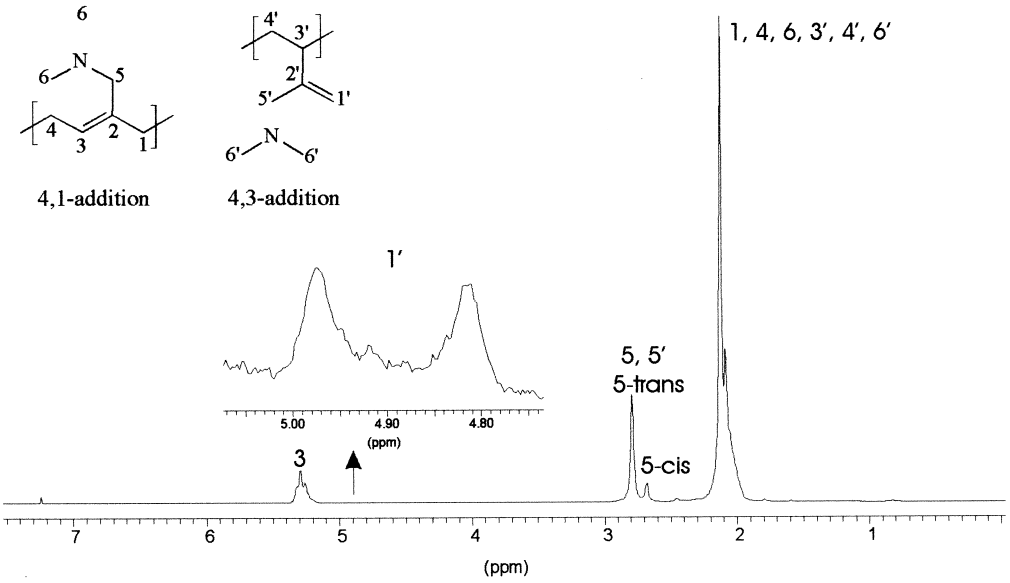

Fig. 4. ^{1}H NMR spectrum of a PDMAi synthezised in toluene at −40°C ($CDCl_3$, 250 MHz).

the vinylic proton of the 4,1-connected monomer. The doublet occurring at 2.70/2.85 ppm is caused by the methylene units adjacent to the amino group. NOE-NMR experiments showed that the less shielded signal at 2.85 ppm has to be assigned to the 4,1-*trans*-addition and the more shielded signal at 2.70 has to be assigned to the 4,1-*cis*-addition [22]. Only at a high magnification of the spectrum, small amounts (1–2%) of 4,3-added units are detectable.

The relative amounts of 4,1-*cis* and 4,1-*trans* addition are found to depend on temperature; keeping all other polymerization parameters fixed, the amount of 4,1-*cis* connected monomer units increases slightly with increasing temperature, whereas the amount of vinyl- (4,3-) linkage does not change within experimental error as can be seen from Table 2.

The microstructure significantly depends on the ratio of monomer/initiator concentration under otherwise identical polymerization conditions. Fig. 5(a) shows the results of a number of polymerizations with different ratios of monomer/initiator. The amount of 4,1-*trans* connected units in the resulting polymers increases with increasing monomer/initiator ratio, i.e. with increasing molecular weight, reaching a limiting value of about 95% 4,1-*trans* connected monomer units at a molecular weight of about 25 kg/mol. This high stereoregularity is best appreciated in ^{13}C NMR spectroscopy (Fig. 5(b)).

Table 2
Temperature dependence of the microstructure

Temperature (°C)	4,1-*trans* (%)	4,1-*cis* (%)	4,3 (%)
−40	83	16	1
−20	80	18	2
+20	74	24	2

4.1.3. Size exclusion chromatography

SEC characterization of these PDMAi is not possible using standard SEC columns filled with crosslinked polystyrene gel. The high basicity of the tertiary aliphatic amine causes complete adsorbtion of the polymer on the column material. Only by using a special polyester gel (gr_am columns from Polymer Standards Service) and THF as eluent, the determination of the molecular weight distributions became possible. Fig. 6 shows a typical SEC trace of a PDMAi having a molecular weight of 75 kg/mol determined by membrane osmometry.

SEC traces are monomodal in all cases and almost symmetrical so that a broadened distribution due to adsorption processes can be ruled out. In all cases comparatively broad molecular weight distributions between 1.2 and 1.4 are obtained. Polydispersities of this range are often found when the initiation of the polymerization is slower than its growth. In all the kinetic studies of the polymerization behavior of 5-(*N*,*N*-dimethylamino)-isoprene, however, there never was any indication for a slow initiation.

4.2. Discussion

Taking into consideration the unusual kinetic behavior of the DMAi polymerization as well as the unexpected high regio- and stereospecificity of the monomer addition and the relatively broad molecular weight distribution of the resulting polymers, a complex growth mechanism has to be assumed. A possible explanation lies in the existence of several differently associated species adding monomer at different rate constants. An association of the living chain end could take place through complexation of amine functionalities of free monomer as well as of already polymerized amine units through the lithium counter ion. If the addition of monomer to these different associated species

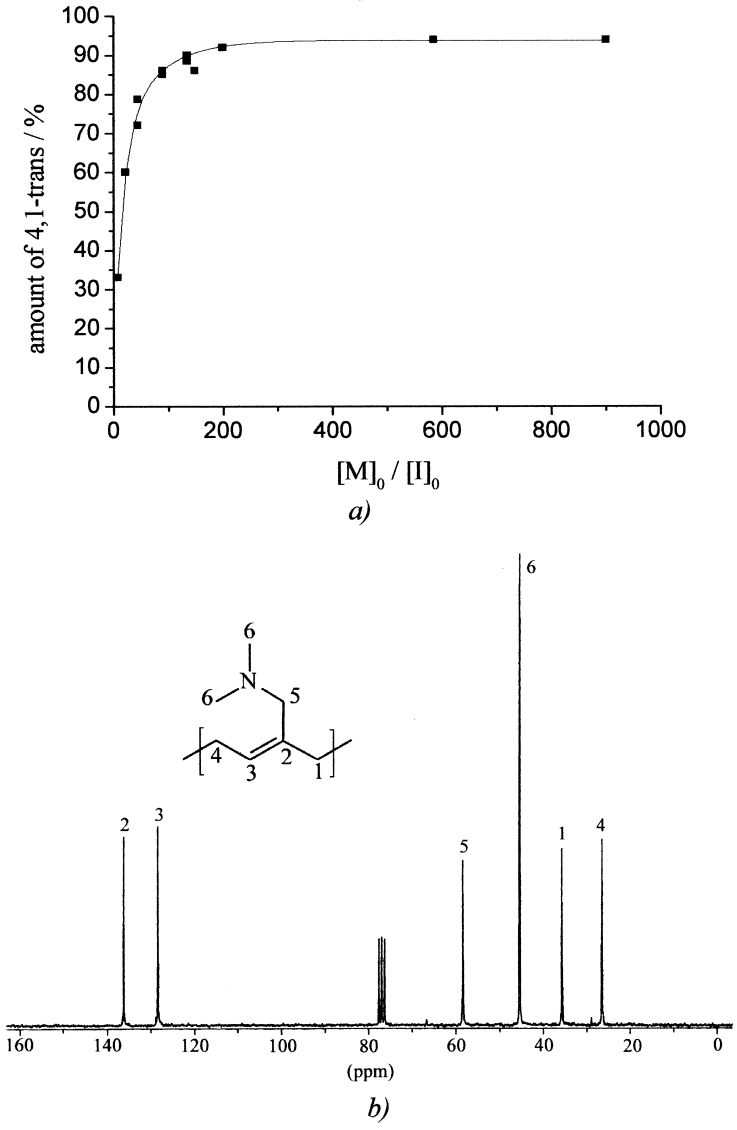

Fig. 5. (a) Dependence of the amount of 4,1-*trans* addition on the ratio monomer/initiator; (b) ^{13}C NMR of PDMAi with 95% 4,1-*trans* addition.

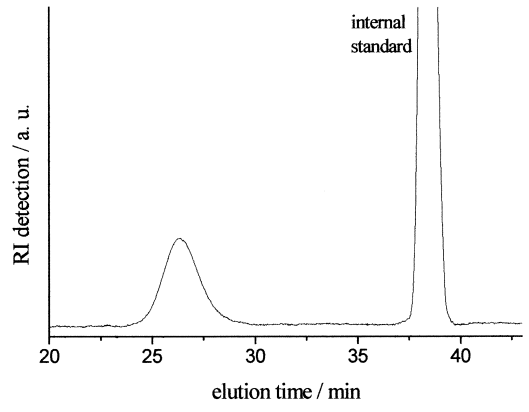

Fig. 6. Typical SEC trace of a poly[5-(*N*,*N*-dimethylamino)-isoprene]; molecular weight: 75 kg/mol (determined by membrane osmometry); polydispersity: 1.29.

was quicker than the interconversion between the species, the resulting molecular weight distribution would broaden as observed. Such a complexation could also explain the high regio- and stereoregularity of monomer addition and the peculiar slow growth in polar solvents.

5. Crystallization behavior of poly[5-(*N*,*N*-dimethylamino)-isoprene] (PDMAi)

The emphasis of the characterization of the poly[5-(*N*,*N*-dimethylamino)-isoprenes] was laid on the crystallization resulting from the high stereoregularity. Although several PDMAi of high molecular weight and almost exclusive 4,1-*trans* microstructure were synthesized, only results on solution cast PDMAi with a molecular weight of 65 kg/mol and 95% 4,1-*trans* units are discussed.

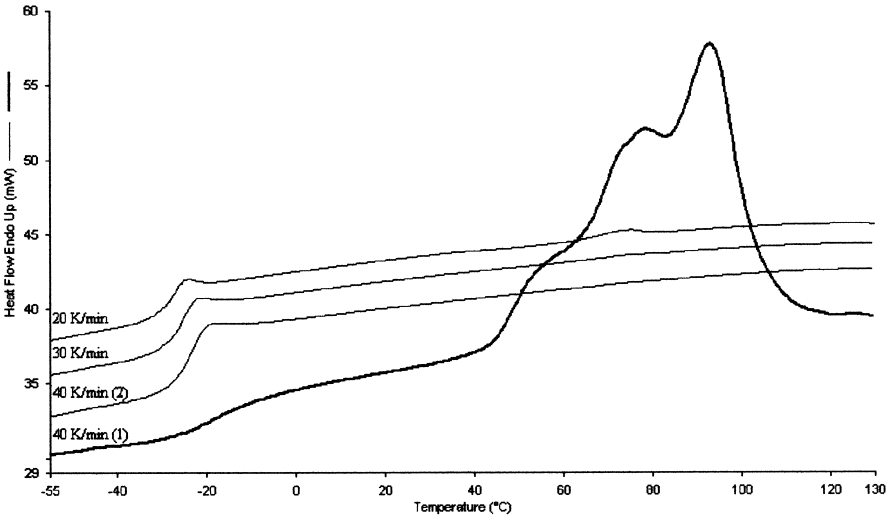

Fig. 7. DSC traces of PDMAi at different heating rates.

5.1. Results

5.1.1. DSC investigations

DSC measurements reveal a glass transition temperature of −30°C (extrapolated to 0 K/min) and a broad melting interval between 50 and 120°C at first heating. By rapid cooling of the sample, the recrystallization can be suppressed completely so that a totally amorphous sample is obtained. This quenching of the sample allows the determination of its degree of crystallinity by determining the corresponding changes in heat capacity of the semicrystalline and the amorphous sample (curves (1) and (2) in Fig. 7). From this analysis, PDMAi with a degree of crystallinity close to 60% is obtained. For a closer investigation of the melting and crystallization behavior of PDMAi, more detailed DSC tests were run. For the annealing experiments the following procedure is employed:

1. *Extinction of thermal history:* the sample is kept at 130°C for 5 min;
2. *Cooling down to the desired recrystallization temperature* T_c: the sample is cooled down to T_c with 10 K/min;
3. *Isothermal crystallization:* the sample is kept at the crystallization temperature T_c until it is completely recrystallized;
4. *Melting:* the sample is heated with 10 K/min from T_c until it is entirely molten (110°C).

Fig. 8 shows the isothermes (step 3) as well as the heating curves (step 4) of PDMAi.

The plot of the isothermes (Fig. 8a) shows that the recrystallization at first proceeds faster with decreasing crystallization temperature T_c but then slows down. This behavior is generally observed in polymer crystallization. On the one hand, on decreasing the crystallization temperature the thermodynamic driving force rises thus accelerating the crystallization, while on the other hand, the viscosity of the polymer melt increases, ultimately reducing the crystallization rate.

With higher crystallization temperatures, a second melting point is observed at reheating (Fig. 8b) although the recrystallization isothermes in all cases show only one, however broad, crystallization peak. This indicates that two different crystallization processes coincide with one crystallization isotherme.

As the melting point of a semicrystalline polymer generally depends on its thermal history, in particular on the crystallization temperature and the employed heating rate, it is useful to determine its equilibrium melting temperature by extrapolation. This can best be done by the method of Hoffman and Weeks [24] using the heating curves in Fig. 8(b). Fig. 9 shows the extrapolation of the two observed melting points onto the straight line where T_m (melting temperature) $= T_c$ (crystallization temperature).

For the determination of the exact equilibrium melting temperatures a correction for the finite heating rate has to be performed. Therefore, for one selected temperature (35°C) the dependence of the heating rate on the obtained melting points is determined by using heating rates of 10, 5, 2, 1, 0.5 and 0.2 K/min and extrapolating to 0 K/min. The error amounts to 2.5 K resulting in a T_m^0 of the higher melting fraction of 77.2°C and for the lower melting fraction of 72.3°C.

5.2. WAXS measurements

With the help of wide angle X-ray scattering the crystallization behavior of PDMAi was further examined. Therefore, a PDMAi film cast from chloroform about 1 mm thick was melted (110°C, 30 min) and allowed to recrystallize at different temperatures for intervals of 20–40 h. Fig. 10 shows the obtained WAXS intensity profiles at four different temperatures i.e. 6, 20, 45 and 60°C.

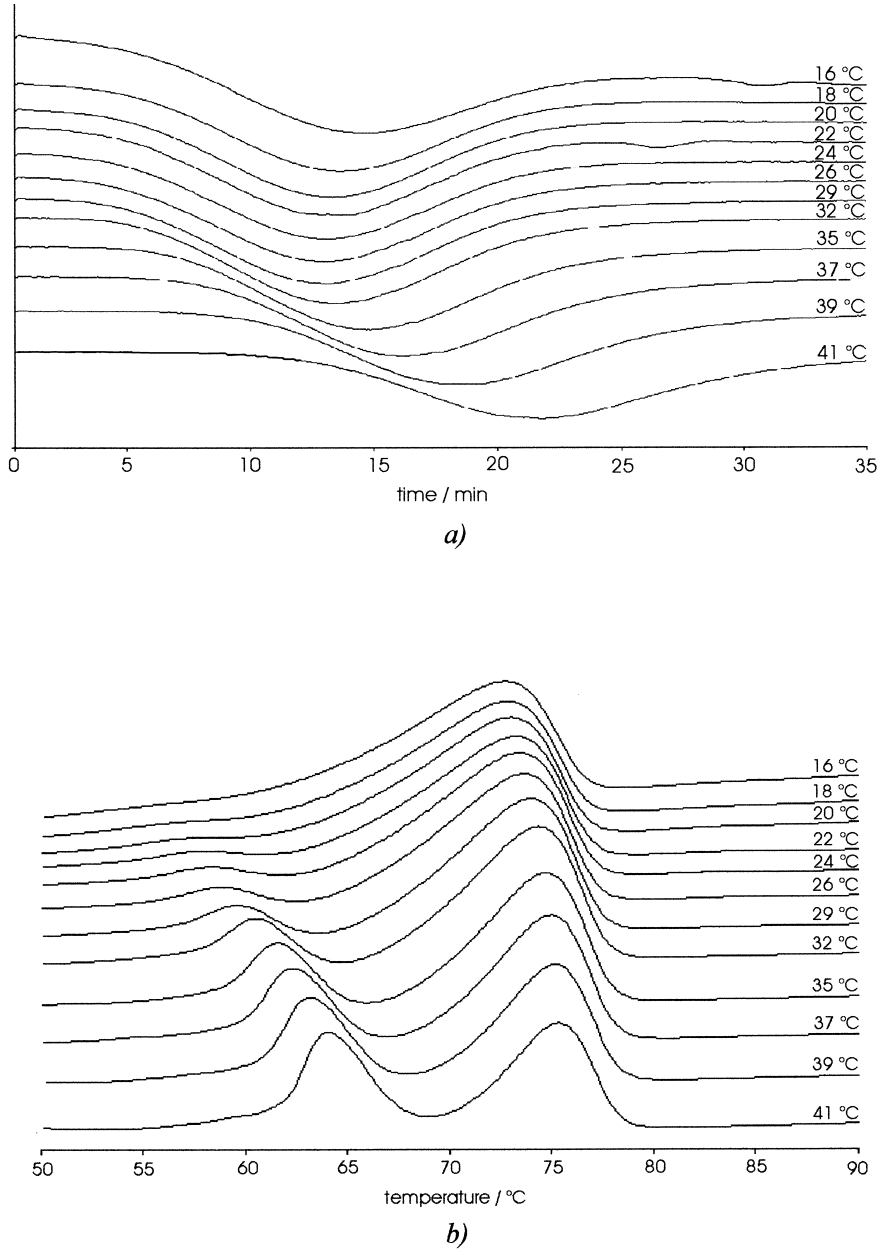

Fig. 8. (a) Isothermes; and (b) Heating curves of PDMAi.

Apart from the fact that the degree of crystallinity is considerably higher at higher crystallization temperatures due to a greater mobility of the polymer chains closer to the melting point, it is clearly seen that two different crystal modifications appear. The arrows in the magnification in Fig. 10 mark reflexes which are more intense in the samples that were recrystallized at low temperatures, where a second crystal modification becomes important.

Efforts to determine the exact crystal structure by indexing the reflexes has not been successful. Although two distinct crystal modifications can be distinguished, they never could be obtained purely. An assignment of the smaller reflexes to one of the two modifications thus turned out to be impossible.

Distinct differences in the WAXS profiles are obtained by different methods of film preparation from solution. Fig. 11(a) shows the profile of a PDMAi sample which was dissolved in *n*-hexane at 50°C and allowed to recrystallize at 6°C. In Fig. 11(b) the profile obtained by film casting from chloroform at room temperature is displayed. The comparison with the profiles obtained by melting and recrystallization at different temperatures shows that the sample obtained on recrystallization in *n*-hexane resembles the one obtained on melting (110°C) and recrystallizing at 60°C, whereas the profile of the chloroform-cast sample shows a greater similarity to the one obtained on melting and recrystallizing at 20°C although it obviously contains larger amounts of the other modification as well.

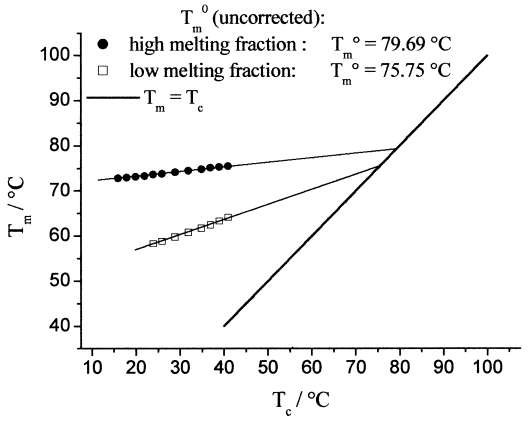

Fig. 9. Determination of (uncorrected) equilibrium melting temperatures T_m^0 following the procedure of Hoffman and Weeks.

5.3. Texture

The occurrence of two different crystal modifications can lead to the formation of two distinct textures as shown e.g. for *trans*-poly(1,4-isoprene) TPI [25,26].

This behavior is indeed observed for semicrystalline PDMAi. Solvent evaporation and crystallization of a drop

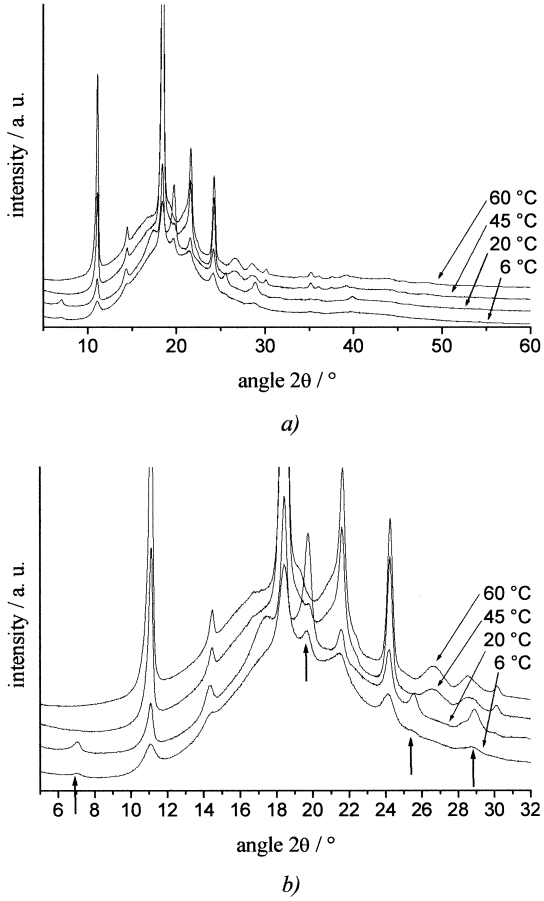

Fig. 10. X-ray diffractogramm of PDMAi after melting and annealing at different temperatures: (a) entire profile; (b) magnification.

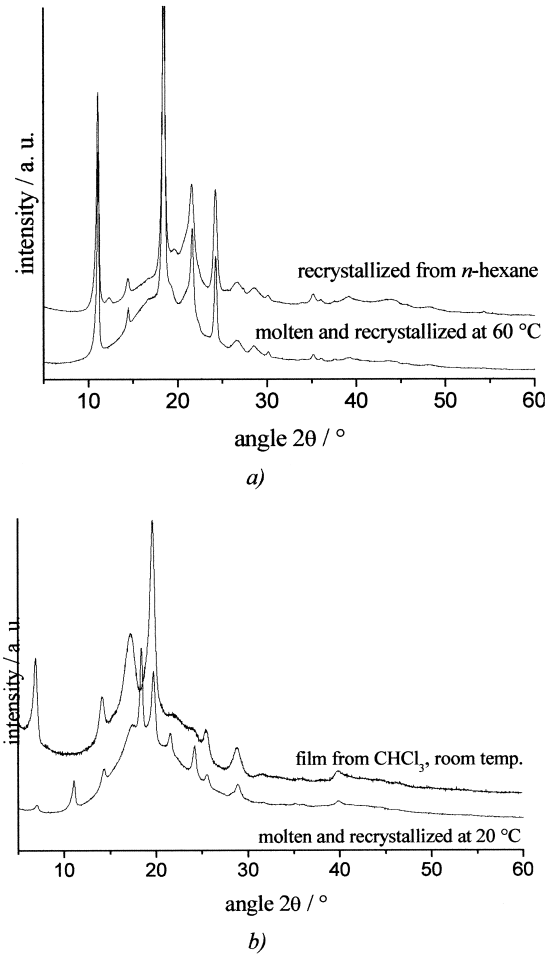

Fig. 11. X-ray diffractogramms of PDMAi: (a) comparison of the film annealed at 20°C with the sample recrystallized from *n*-hexane; and (b) comparison of the film annealed at 60°C with the chloroform-cast film.

of a 5% chloroform solution of PDMAi on a microscopy glass slide at room temperature results in cross-polarized optical micrographs as shown in Fig. 12. The question why in some cases this procedure exclusively yields the fine crystalline structures of Fig. 12(a), whereas in other cases also up to 50 μm large spherulites with Maltese cross are formed (Fig. 12(b), cannot be explained conclusively. It may depend on the local concentration of the solution and the rate of evaporation of the solvent as well as on heterogenieties on the glass slide acting as nucleation sites.

A more detailed characterization of the fine crystalline structure was achieved with the help of AFM. Therefore, the sample from the optical microscopy investigations was examined in the tapping mode. The small magnification in Fig. 13 (10 μm) shows that the crystal growth proceeds in a spherical way; in the higher magnification of a spherulite rim one can clearly see the radially running crystal lamellae and their merging into one another. This proves the existence of spherulites which are too small for detection by light microscopy.

For the determination of the morphology of the polymer

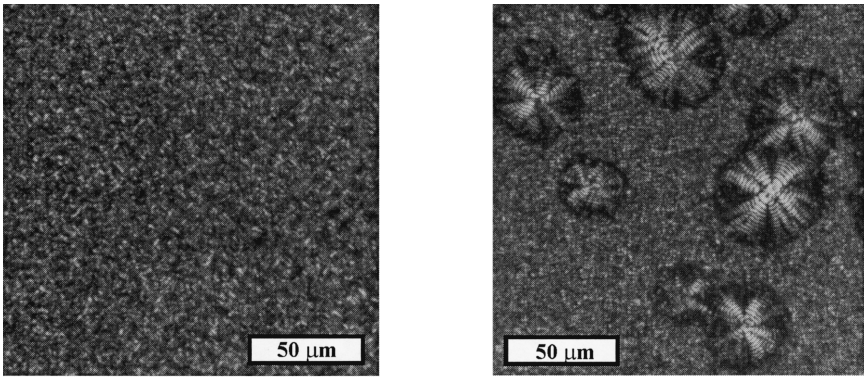

Fig. 12. Cross-polarized optical micrographs of PDMAi; films cast from chloroform.

chains in the semicrystalline PDMAi, thin cuts were examined via TEM after staining with osmium tetroxide. A film of PDMAi (about 1 mm thick) was also investigated by SAXS. For both techniques chloroform-cast films (5% solution by weight) were used. The results are shown in Fig. 14.

The TEM micrograph shows a lamellar structure of the sample which arises because the polymer chain in the crystalline regions of the polymer folds forth and back in a regular way. The lamellar thickness was determined from this micrograph to be about 10 nm. A more exact value was obtained from SAXS measurements; the electron density difference between amorphous and crystalline regions of the sample is high enough to get sufficient scattering intensity. The SAXS intensity profile in Fig. 14(b) shows a broad reflex with its maximum corresponding to a lamellar distance of $d = \lambda/2 \sin \theta = 13.5$ nm ($\lambda = 0.154$ nm).

If the structure from Fig. 12(b) is heated at 5 K/min to 100°C, one observes the melting of the fine crystalline structure at about 75°C while the large ringed spherulites do not melt until a temperature of about 82°C is reached. These melting points agree well with the ones obtained from DSC experiments (72.3 and 77.2°C) if one takes into consideration the error due to the finite heating rate. Thus it is possible to distinguish between the two different crystal modifications by optical microscopy. Fig. 15(a) shows the sample at room temperature and Fig. 15(b) shows the sample after heating to 75°C. Because the birefringence of the large ringed spherulites turned out to be rather low, a compensator (λ-plate; retardation 550 nm) was used for contrast enhancement.

Another proof via optical microscopy for the existence of two modifications having different melting points is shown in Fig. 16. The structure shown here is obtained from a sample identical with the one in Fig. 12(b) (fine crystalline

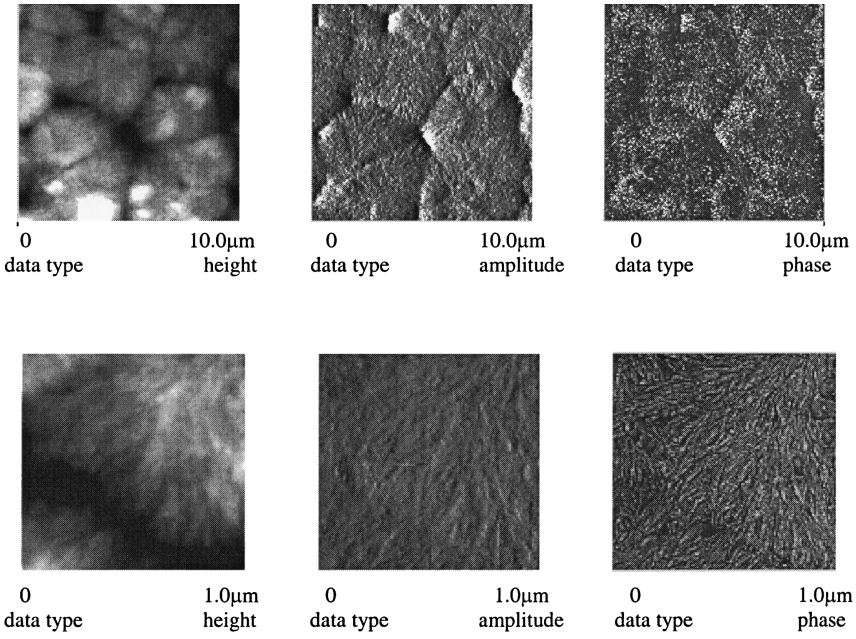

Fig. 13. AFM micrographs of PDMAi; films cast from chloroform.

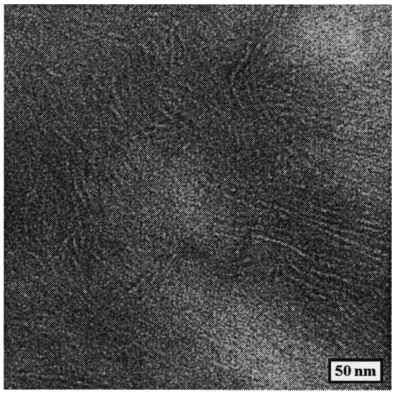

a)

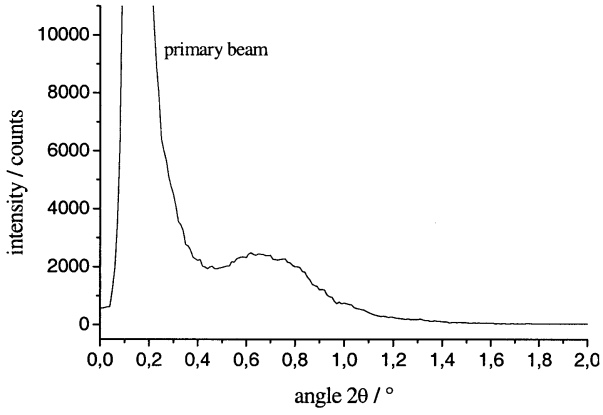

b)

Fig. 14. (a) TEM micrograph and (b) SAXS (CuK_{α}-radiation) of semicrystalline PDMAi.

structure and large ringed spherulites) after heating to 77°C and holding at 65°C for 2 days. This experiment again proves the existence of two different crystal modifications with two different melting temperatures which crystallize into two different textures. The modification which can only be obtained in a fine crystalline structure from solution can be annealed after melting at a temperature close to its melting point in a way that large spherulites are obtained. Fig. 17 shows micrographs of a sample with a fine crystalline structure identical with the one presented in Fig. 12(a). If this structure is melted and allowed to recrystallize at a temperature close to the melting point, i.e. closer to thermal equilibrium, large spherulites showing a distinct birefringence and a radial running dendritic pattern are obtained.

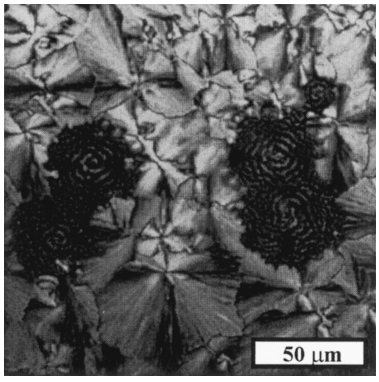

Fig. 16. Chloroform-cast film of PDMAi after heating to 77°C and annealing at 65°C for 2 days to allow for recrystallization.

If such samples are recrystallized at lower temperatures the spherulite size decreases; at room temperature the structure is identical with the one obtained from solution-cast samples. This second modification preferentially forms when crystallization takes place from solution at low temperatures. Fig. 18 shows the result of a sample which was cast at 6°C from chloroform. Here the large ringed spherulites showing a marked Maltese cross dominate. Using the λ-plate again shows that this modification is substantially less birefringent than the small spherulites of the first modification.

6. Discussion

A comparison of the crystallization behavior of PDMAi

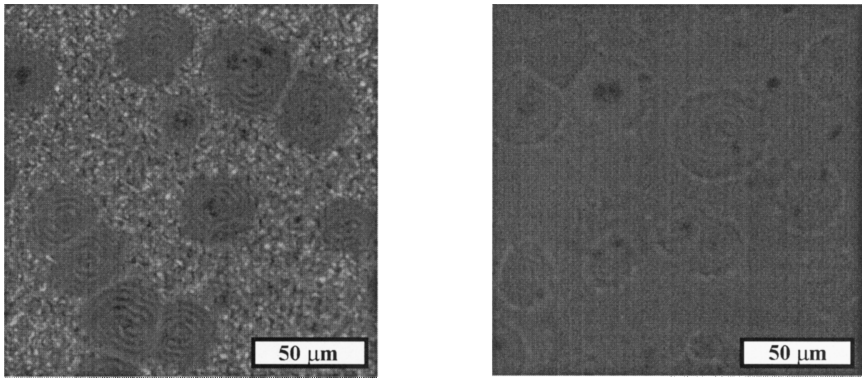

a) b)

Fig. 15. Optical micrographs using crossed polarizers and λ-plate of PDMAi: (a) film from $CHCl_3$; and (b) after heating to 75°C.

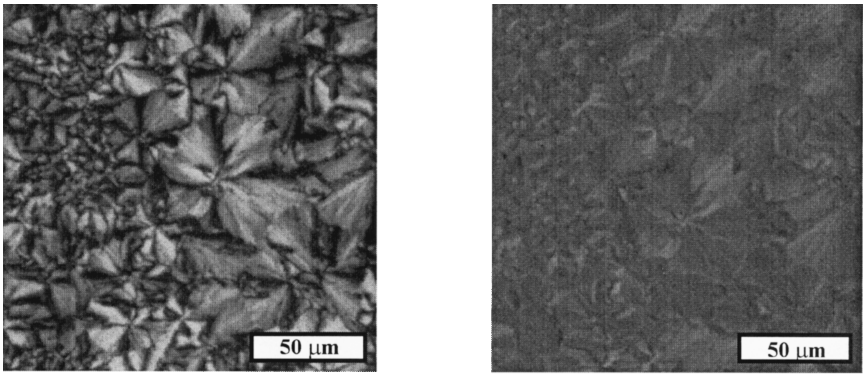

a) b)

Fig. 17. (a) Chloroform-cast film of PDMAi after heating to 100°C and holding at 60°C for 2 days to allow for recrystallization; and (b) with λ-plate.

with *trans*-polyisoprene (TPI) shows great similarities. TPI shows similar degrees of crystallinity [27–29] and also crystallizes in two different crystal modifications [24,26,30–35,40] exhibiting two different melting points [36–40] and two distinct spherulitic textures [25,26] are described. Investigation of TPI at room temperature yields a long period of the same order of magnitude as found for PDMAi (13.5 nm from SAXS) of about 15 nm [28].

The results of the DSC and WAXS investigations in combination with the literature data of TPI enables the assignment of the two modifications.

The fine crystalline, highly birefringent structure observed in cross-polarized light microscopy experiments (where only through AFM a spherulitic structure can be proven) can be obtained as larger spherulites showing a Maltese cross without ringing and a dendritic pattern if annealing experiments at higher temperatures are performed. These spherulites have a melting temperature of about 75°C as determined from light microscopy experiments on a hot stage which agrees well with the melting temperature of the second melting point appearing in DSC measurements at higher crystallization temperatures of 72.3°C. Therefore, this structure is identified as the low melting form (LMF) in analogy to the corresponding modification of TPI.

The strongly ringed large spherulites with Maltese cross and low birefringence have a melting temperature observed in cross-polarized light microscopy experiments on the hot stage of approximately 82°C which compares well with the melting point of 77.2°C found in DSC measurements. Therefore, this structure corresponds to the high melting form (HMF). In agreement with the results from DSC it was shown by optical microscopy that the HMF preferentially forms at low crystallization temperatures. The HMF could never be obtained from the melt. This is consistent with the results from WAXS measurements where the second modification only appears in small amounts after melting and recrystallization at different temperatures.

7. Conclusions

We have studied the kinetics of the *sec*-butyllithium initiated anionic polymerization of 5-(*N*,*N*-dimethylamino)-isoprene (DMAi) in toluene as well as the microstructure of the obtained polymers and their dependence on temperature and molecular weight. Polymerization

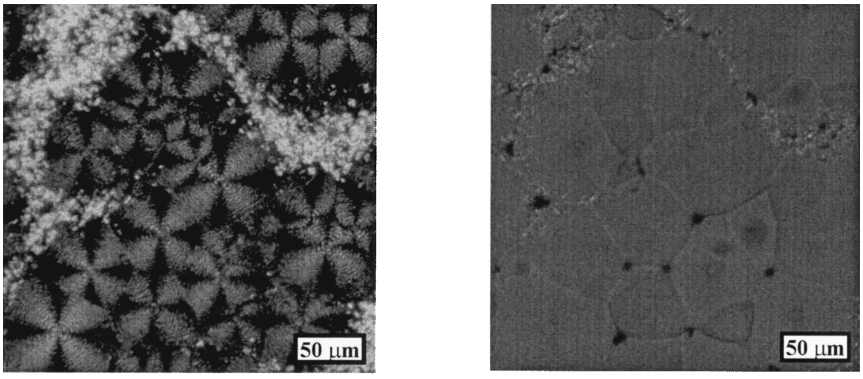

a) b)

Fig. 18. PDMAi: (a) chloroform-cast at 6°C; and (b) using a λ-plate.

conditions resulting in almost exclusive 4,1-*trans* addition of monomer were found. The so synthezised polymers are semicrystalline with degrees of crystallinity of about 55–60% and show polymorphic behavior. DSC experiments reveal two melting points at 72.3 and 77.2°C with the relative amount of the LMF increasing with higher crystallization temperature. WAXS intensity profiles of PDMAi films show two different crystal modifications depending on the condition of film preparation. Under cross-polarized light both modifications can be distinguished because they form different spherulitic textures.

The comparison with TPI shows that the PDMAi with 95% 4,1-*trans* connected units shows properties very similar to TPI. Both polymers possess equal degrees of crystallinity; they both show polymorphism and with DSC, WAXS and cross-polarized light microscopy the two crystal modifications can be distinguished. Although the identification of the crystal modifications of PDMAi by WAXS was not possible they are found to be somewhat similar to the ones observed in TPI as far as melting points and textures are concerned.

Acknowledgements

The authors are deeply indebted to R. Stadler who initiated this work. R.B. thanks L. Braun and A. Krökel for kindly supplying the monomer, A. Göpfert for the TEM measurements and N. Rehse (Physikalische Chemie II, Universität Bayreuth) for the AFM investigations. Financial support by DFG (STA 272/6-2, AB 113/1-3) and the Bayreuther Institut für Makromolekülforschung (BIMF) is gratefully acknowledged.

References

[1] Hsieh HL, Quirk RP. Anionic polymerization—principles and practical applications. New York: Marcel Dekker, 1996.
[2] Stavely FW, Forster FC, Binder LL, Forman LE. Ind Engng Chem 1956;48:778.
[3] Hsieh H, Tobolsky AV. J Polym Sci 1957;25:245.
[4] Bywater S. Adv Polym Sci 1965;4:66.
[5] Tobolsky AV, Rogers CE. J Polym Sci 1959;40:73.
[6] Bywater S. In: Eastmond IGC, Ledwith A, Russo S, Sigwalt P, editors. Comprehensive polymer science, Chain polymerization, vol. 3. Elmsford, NY: Pergamon Press, 1989. p. 433 (chap. 28).
[7] Hsieh H, Kelley DJ, Tobolsky AV. J Polym Sci 1957;26:240.
[8] Salle R, Pham QT. J Polym Sci Polym Chem Ed 1977;15:1799.
[9] Langer Jr AW. Am Chem Soc, Div Polym Chem Prep 1966;7(1):132.
[10] Essel A, Salle R, Gole J, Pham QTJ. Polym Sci Polym Chem Ed 1971;13:1847.
[11] Antkowiak TA, Oberster AE, Halasa AF, Tate DP. J Polym Sci Part A-1 1972;10:1319.
[12] Halasa AF, Lohr DF, Hall JE. J Polym Sci Polym Chem Ed 1981;19:1357.
[13] Bywater S, Mackerron DH, Worsfold DJ. J Polym Sci Polym Chem Ed 1985;23:1997.
[14] Endo K, Takakura Y, Otsu T. Polym Int 1998;45:414.
[15] Ohno R, Tanaka Y, Kawakami M. Polym J 1973;4:56.
[16] Suzuki T, Tsuji Y, Tkegami Y. Macromolecules 1978;11:639.
[17] Suzuki T, Tsuji Y, Tkegami Y, Harwood H. Macromolecules 1979;12:235.
[18] Ding Y-X, Weber WP. Macromolecules 1988;21:532.
[19] Takenaka K, Hirao A, Hattori T, Nakahama S. Macromolecules 1987;20:2035.
[20] Takenaka K, Hattori T, Hirao A, Nakahama S. Macromolecules 1989;22:1563.
[21] Hirao A, Hiraishi Y, Nakahama S, Takenaka K. Macromolecules 1998;31:281.
[22] Petzhold C. PhD thesis, Mainz, Germany, 1994.
[23] Mannebach G, Morschhäuser R, Stadler R, Petzhold C. Macromol Chem Phys 1998;199:909.
[24] Wunderlich B. Macromolecular physics, Crystal melting, vol. 3. New York: Academic Press, 1976. p. 33.
[25] Schuur G. Polym Sci 1953;11:385.
[26] Fischer E, Henderson JF. J Polym Sci Part A-2 1967;5:377.
[27] Hardin IR, Yeh GSYJ. Macromol Sci 1973;B7:375.
[28] Hardin IR, Yeh GSYJ. Macromol Sci 1973;B7:393.
[29] Boochathum P, Shimizu M, Mita K, Tanaka Y. Polymer 1993;34:2564.
[30] Corrigan JP, Zemel IS, Woodward AE. J Polym Sci Polym Phys Ed 1989;27:1135.
[31] Boochathum P, Tanaka Y, Okuyama K. Polymer 1993;34:3694.
[32] Mandelkern L, Quinn Jr. FA, Roberts DE. J Am Chem Soc 1956;78:926.
[33] Bunn CW. Proc R Soc London, Sect A 1942;180:40.
[34] Fisher D. Proc Phys Soc London, Sect B 1953;66:7.
[35] Takahashi Y, Sato T, Tadokoro H, Tanaka Y. J Polym Sci Polym Phys Ed 1973;11:233.
[36] Cooper W, Vaughan G. Polymer 1963;4:329.
[37] Flanagan RD, Rijke AM. J Polym Sci Part A-2 1972;10:1207.
[38] Cooper W, Smith RK. J Polym Sci Part A 1963;1:159.
[39] Davies CKL, Long OEJ. J Mater Sci 1979;14:2529.
[40] Boochathum P, Tanaka Y, Okuyama K. Polymer 1993;34:3699.